Available online at www.sciencedirect.com
ScienceDirect
Journal of Sound and Vibration 321 (2009) 721–734
JOURNAL OF SOUND AND VIBRATION
www.elsevier.com/locate/jsvi

Vibration of a truss structure excited by a moving oscillator

Luis Baeza[a], Huajiang Ouyang[b,*]

[a] *Dpto. de Ingeniería Mecánica, Universidad Politécnica de Valencia, Camino de Vera s/n, 46022 Valencia, Spain*
[b] *Department of Engineering, University of Liverpool, Liverpool L69 3GH, UK*

Received 7 April 2008; received in revised form 27 August 2008; accepted 27 September 2008
Handling Editor: A.V. Metrikine
Available online 13 November 2008

Abstract

This paper studies the vibration of a truss structure composed of a number of rigidly connected Timoshenko beams. The excitation is provided by a moving oscillator of an unsprung mass that supports another mass through a spring (oscillator) and moves on top of the truss structure. Each component beam of the structure is meshed with a number of Timoshenko beam elements. The finite-element (FE) modes of the whole structure are first obtained for the nodes of the FE mesh and then they are converted into an analytical form that is constructed over all the elements of the top deck of the truss through the element shape functions, whereby the location of the moving oscillator is easily tracked and the displacement continuity and force equilibrium conditions at the contact point can be easily implemented. This numerical–analytical combined approach has the advantage of the versatility of the FE method in dealing with structures (trusses or frames in this paper) of arbitrary configurations and the special efficiency and convenience of the analytical method in dealing with moving loads. Vibration of the truss structure and vibration of the oscillator are studied through simulated examples. It is found that the dynamic response can be several times higher than the relevant static response at high speeds. It is also found that the dynamic contact force can be much higher than its static value and may become negative if the contact between the oscillator and the truss is assumed to be constantly maintained. Interestingly, suitably chosen parameter values can bring the dynamic response and the dynamic contact force close to their respective static values.

1. Introduction

Vibration of a stationary structure excited by another structure moving on the surface of the stationary structure is very common in engineering, such as vibration of bridges or railway track under travelling vehicles. In the simplest case, the moving structure may be modelled as a constant force or a mass or an oscillator while the stationary structure may be modelled as a single or continuous beam [1–4] or any of these on a viscous-elastic foundation [5]. Analytical solutions of simple moving-load problems can be found in Frýba's monograph [6]. For a moving flexible body [7], numerical methods must be used.

Model refinement can be made to the moving structure or the stationary structure or both to better represent real structures. In the case of the moving structure, a train was modelled as a two-axle mass-spring-damper

*Corresponding author. Fax: +44 151 794 4848.
E-mail address: h.ouyang@liverpool.ac.uk (H. Ouyang).

0022-460X/$ - see front matter
doi:10.1016/j.jsv.2008.09.049

system supporting a rigid body in Refs. [8,9] and as a system of multiple oscillators in Ref. [10]. As for the stationary structure, various types of bridges were studied by a number of researchers [11–18]. There is a wealth of publications on vehicle–bridge interaction. Interested readers should also refer to the comprehensive review paper by Au et al. [18]. The monograph by Yang et al. [19] also provides an in-depth study of vehicle–bridge interaction dynamics.

Many bridges are made from pin-connected or rigidly-connected (through welding or bolted joints) beams in various configurations. The vibration of a bridge in the form of a simple plane frame excited by moving loads was studied in Ref. [12]. A plane truss structure excited by a moving oscillator is the subject of this paper. As shear may be important in many cases, Timoshenko beam theory [20] is used. A mass in contact with the stationary structure and supporting another mass through a spring as a simplistic representation of a vehicle is the model for the moving structure and is referred to as a moving oscillator. A regular finite element (FE) mesh is used for each beam component for the truss structure studied in this paper. Numerical modes and frequencies of the truss are obtained using MATLAB. For more complicated structures, an adaptive FE mesh [21] may be used. The modes obtained for the nodes of the mesh are then replaced with analytical forms for mathematical convenience and numerical efficiency in solving this moving-load problem. The equations of motion for the whole system are solved numerically for efficiency. The computing code is capable of automatically generating a number of typical truss configurations. To the authors' best knowledge, dynamic interaction between a truss structure and a moving oscillator has not been studied in the past. The difference between the horizontal location of the moving oscillator and the actual coordinate of the supporting structure caused by the axial motion and the beam rotation is investigated for the first time.

2. Theoretical basis of the numerical–analytical methodology

It is known that even for a single-span beam with classical boundary conditions higher frequencies and modes are very sensitive to small errors inherent in the calculation using the analytical method [22,23] and hence are difficult to determine accurately. The main reason is that the exponential functions in a high (analytical) beam mode produce huge numbers and the transcendental equation in the natural frequencies of the beam becomes increasingly ill-conditioned. So for the sake of both accuracy and versatility (in modelling various configurations of structures), the FE method is used to obtain the modes at first. When the number of the finite elements used is sufficient, the FE modes will be very close to the analytical modes and can be considered a substitute of the analytical modes after conversion using the element shape functions.

It is demonstrated in Appendix A that the analytical modes of a continuous Euler beam resting on three supports are orthogonal. For more complicated structures, such as the truss structure shown in Fig. 1, orthoganality of the analytical modes should still hold but are difficult to demonstrate.

The equations of free vibration of each component beam modelled as a Timoshenko beam in its local coordinate ξ are [20]

$$\rho A\frac{\partial^2 w}{\partial t^2}-\frac{\partial}{\partial \xi}\left[\gamma GA\left(\frac{\partial w}{\partial \xi}-\theta\right)\right]=0$$

$$\rho I\frac{\partial^2 \theta}{\partial t^2}-\frac{\partial}{\partial \xi}\left(EI\frac{\partial \theta}{\partial \xi}\right)-\gamma GA\left(\frac{\partial w}{\partial \xi}-\theta\right)=0 \tag{1}$$

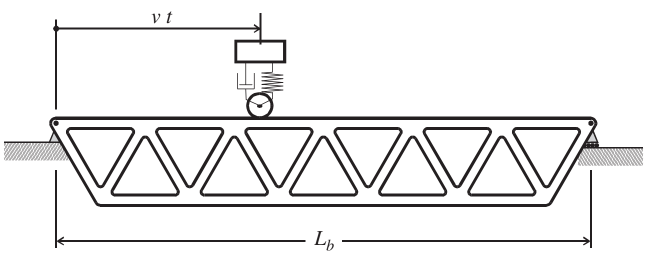

Fig. 1. A truss made of rigidly connected beams.

where w and θ are the transverse displacement and the rotation of the cross-section of the beam, E, G and γ are Young's modulus, shear modulus and shear factor, ρ is the mass density, A and I are the area and second moment of area of the beam cross-section. Denote the analytical w-component and θ-component modes of the k-th beam as $\psi_{wk}(\xi)$ and $\psi_{\theta k}(\xi)$, which consist of base functions of sin, co-sin, hyper-sin and hyper-co-sin functions when expressed exactly [24]. Through the displacement continuity and equilibrium conditions at the joints where more than one component beam meets, a matrix equation in the coefficients of the base functions for all the beams can be derived. Natural frequencies of the whole structure can be computed in theory from the equation that the determinant of the above matrix vanishes. However, this determinant equation is a highly transcendental one and hence it is very difficult to actually solve accurately. This difficulty can be appreciated from a simpler problem of computing higher frequencies and modes of an Euler beam [23]. Naturally the FE method presents a simple and versatile way of computing the frequencies and modes of a structure of arbitrary configuration and hence is used.

On the other hand, there is a big advantage of using an analytical formulation for a moving-load problem in that when a load moves in the spatial domain, its location always corresponds to a degree-of-freedom (a continuous coordinate) in an analytical formulation. This allows easy enforcement of displacement continuity and force equilibrium of the moving and stationary bodies at the moving coordinate. In contrast, in an FE formulation, the moving load is located in different element domains at different time, hence it is difficult to track its location constantly and in particular relate its motion to that of the FE nodal displacement vector as it traverses different element domains. Apparently, the numerical procedure for a moving-load problem using the FE method is more complicated and less accurate than using an analytical method, if the latter affords an analytical expression of modes.

The arguments in the above two paragraphs poses a dilemma: the advantage of using analytical method in dealing with moving loads and the advantage of using the FE method in determining the frequencies and modes. A numerical–analytical combined approach is put forward, which takes advantages of both methods. Each component beam is divided into a number of Timoshenko beam elements [25]. The frequencies and modes are obtained by the FE method. Denote the n-th numerical mode $\boldsymbol{\psi}_n^{\mathrm{FE}}$ of the truss structure as $\{w_1, \theta_1, w_2, \theta_2, \ldots, w_i, \theta_i, w_{i+1}, \theta_{i+1}, \ldots\}_n^{\mathrm{T}}$, where subscript i denotes the left node of the i-th beam element and the right node of the ($i-1$)-th beam element, and superscript T stands for matrix transpose. When the number of beam elements is sufficient, the numerical modes and frequencies will be very close to the exact (analytical) modes and frequencies of the whole structure. Denote the i-th element shape function matrix for w-displacement by $\mathbf{N}_{wi}(\xi)$. Then one gets an approximate expression of the n-th analytical mode of the top deck as

$$\psi_{wn}(x) = \begin{cases} \mathbf{N}_{w1}(\xi_1)\{w_1, \theta_1, w_2, \theta_2\}^{\mathrm{T}} & \text{when } \xi_1 \text{ within element 1 domain} \\ \mathbf{N}_{w2}(\xi_2)\{w_2,\ \theta_2,\ w_3,\ \theta_3\}^{\mathrm{T}} & \text{when } \xi_2 \text{ within element 2 domain} \\ & . \\ & . \\ & . \\ \mathbf{N}_{wi}(\xi_i)\{w_i, \theta_i, w_{i+1}, \theta_{i+1}\}^{\mathrm{T}} & \text{when } \xi_i \text{ within element } i \text{ domain} \\ & . \\ & . \\ & . \end{cases} \tag{2}$$

where ξ_i is the local horizontal coordinate of the i-th element in the top deck. This procedure of converting numerical modes to the approximate analytical modes also works for $\theta(x, t)$ and any other displacements.

The equation motion of the truss subjected to the dynamic contact force f_c from the moving oscillator by the FE method is

$$\mathbf{M}\ddot{\mathbf{u}} + \mathbf{K}\mathbf{u} = \mathbf{f} \tag{3}$$

where $\mathbf{M}$ and $\mathbf{K}$ are the mass and stiffness matrices of the truss, $\mathbf{u}$ and $\mathbf{f}$ are, respectively the nodal displacement vector and force vector of the truss. The dot over a symbol represents differentiation with respect to time t.

Only the vertical forces and bending moments at the left node and the right node of the element where f_c is acting instantaneously are not zero and the rest of $\mathbf{f}$ are zero. The nodal displacement vector of the whole structure can be expressed as

$$\mathbf{u}(t) = \sum_n \boldsymbol{\psi}_n^{\mathrm{FE}} q_n(t) = \boldsymbol{\Psi}\mathbf{q}(t) \tag{4}$$

where $q_n(t)$ is the n-th modal coordinate of the truss structure and vector $\mathbf{q}(t) = \{q_1(t), q_2(t), \ldots, \}^{\mathrm{T}}$, $\boldsymbol{\psi}_n^{\mathrm{FE}}$ is the n-th FE mode of the truss structure and $\boldsymbol{\Psi}$ is formed by a number of $\boldsymbol{\psi}_n^{\mathrm{FE}}$ (in the order of ascending frequencies).

3. Kinematics of the moving load in relation to the truss

During vibration, a beam moves to a new location due to its axial motion. In addition, the cross-section of a beam rotates. As a result of both motions, a point on the top fibre of the beam at x now becomes x^*, in the un-deformed coordinate system, as shown in Fig. 2. Hochlenert [26] considered position surface loads due to the rotation of the cross-section of a moving beam and a rotating disc. The kinematic relationship between its un-deformed location and the deformed one of the same point is

$$x^* = vt = x + u(x,t) - h\theta(x,t) \tag{5}$$

where u is the axial displacement and h is half of the beam height.

The mass-normalised FE modes for the horizontal displacement components, the vertical displacement components and the rotation components of the cross-section of the beam in the top deck are denoted by $\boldsymbol{\psi}_u^{\mathrm{FE}}$, $\boldsymbol{\psi}_w^{\mathrm{FE}}$ and $\boldsymbol{\psi}_\theta^{\mathrm{FE}}$, respectively. It follows that these three displacements at the top deck can be expressed as

$$[u(x,t)\ \ w(x,t)\ \ \theta(x,t)] = \mathbf{q}^{\mathrm{T}}(t)[\boldsymbol{\psi}_u(x)\ \ \boldsymbol{\psi}_w(x)\ \ \boldsymbol{\psi}_\theta(x)] \tag{6}$$

where $\boldsymbol{\psi}_u(x)$, $\boldsymbol{\psi}_w(x)$ and $\boldsymbol{\psi}_\theta(x)$ are approximate analytical u-component, w-component and θ-component modes converted from $\boldsymbol{\psi}_u^{\mathrm{FE}}$, $\boldsymbol{\psi}_w^{\mathrm{FE}}$ and $\boldsymbol{\psi}_\theta^{\mathrm{FE}}$ through element shape functions.

In each beam element in the top deck, a new local, non-dimensional coordinate ξ (it should not be confused with the old dimensional local coordinate used in Eqs. (1) and (2)) is defined for the interval $[-1, 1]$, thus $x = x_i + (L/2)(1+\xi)$ where x_i is the x-coordinate of the left-hand side node of the element and L is the length of a beam element. The n-th analytical mode shape function for the i-th element can be approximately expressed through the local coordinate as follows:

$$\psi_{un} = a_{un} + \xi b_{un} \tag{7}$$

$$\psi_{wn} = a_{wn} + \xi b_{wn} + \xi^2 c_{wn} + \xi^3 d_{wn} \tag{8}$$

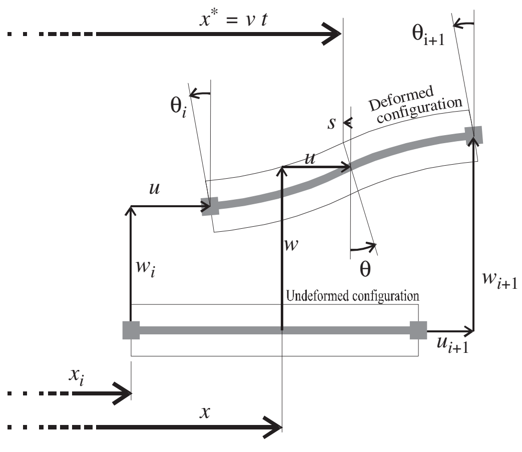

Fig. 2. Kinematics of the beam finite-element.

$$\psi_{\theta n} = a_{\theta n} + \xi b_{\theta n} + \xi^2 c_{\theta n} \tag{9}$$

where the polynomial coefficients (a_{un}, b_{un}, a_{wn}, $b_{wn}, \ldots$) are different in each element. Substituting Eqs. (6)–(9) into (5), one gets

$$x^* = vt = x_i + \frac{L}{2}(1+\xi) + \mathbf{q}^{\mathrm{T}} \begin{pmatrix} a_{u1} + ha_{\theta 1} + \xi(b_{u1} + hb_{\theta 1}) + \xi^2 hc_{\theta 1} \\ a_{u2} + ha_{\theta 2} + \xi(b_{u2} + hb_{\theta 2}) + \xi^2 hc_{\theta 2} \\ \vdots \\ a_{uj} + ha_{\theta j} + \xi(b_{uj} + hb_{\theta j}) + \xi^2 hc_{\theta j} \end{pmatrix} \tag{10}$$

where j is the number of modes used in the subsequent computations. Eq. (10) can be re-ordered, and written in a quadratic equation in ξ below:

$$x_i + \frac{L}{2} - vt + (\mathbf{a}_u^{\mathrm{T}} + h\mathbf{a}_\theta^{\mathrm{T}})\mathbf{q} + \xi\left\{\frac{L}{2} + (\mathbf{b}_u^{\mathrm{T}} + h\mathbf{b}_\theta^{\mathrm{T}})\mathbf{q}\right\} + \xi^2 h\mathbf{c}_\theta^{\mathrm{T}}\mathbf{q} = 0 \tag{11}$$

where ξ and then the coordinate of the contact point x can be computed, and $\mathbf{a}_u = \{a_{u1}, a_{u2}, \ldots, a_{uj}\}^{\mathrm{T}}$, $\mathbf{a}_\theta = \{a_{\theta 1}, a_{\theta 2}, \ldots, a_{\theta j}\}^{\mathrm{T}}$, $\mathbf{b}_u = \{b_{u1}, b_{u2}, \ldots, b_{uj}\}^{\mathrm{T}}$, $\mathbf{b}_\theta = \{b_{\theta 1}, b_{\theta 2}, \ldots, b_{\theta j}\}^{\mathrm{T}}$ and $\mathbf{c}_\theta = \{c_{\theta 1}, c_{\theta 2}, \ldots, c_{\theta j}\}^{\mathrm{T}}$ are determined from the values of the FE modes. Taking differentiations with respect to time once and twice gives

$$-v + (\mathbf{a}_u + h\mathbf{a}_\theta + \xi(\mathbf{b}_u + h\mathbf{b}_\theta) + \xi^2 h\mathbf{c}_\theta)^{\mathrm{T}}\dot{\mathbf{q}} + \left\{\frac{L}{2} + (\mathbf{b}_u + h\mathbf{b}_\theta + 2\xi h\mathbf{c}_\theta)^{\mathrm{T}}\mathbf{q}\right\}\dot{\xi} = 0, \tag{12}$$

$$\begin{aligned} &(\mathbf{a}_u^{\mathrm{T}} + h\mathbf{a}_\theta^{\mathrm{T}} + \xi(\mathbf{b}_u^{\mathrm{T}} + h\mathbf{b}_\theta^{\mathrm{T}}) + \xi^2 h\mathbf{c}_\theta^{\mathrm{T}})\ddot{\mathbf{q}} + (2\dot{\xi}(\mathbf{b}_u^{\mathrm{T}} + h\mathbf{b}_\theta^{\mathrm{T}}) + 4\dot{\xi}\xi h\mathbf{c}_\theta^{\mathrm{T}})\dot{\mathbf{q}} \\ &\quad + 2\dot{\xi}^2 h\mathbf{C}_\theta^{\mathrm{T}}\mathbf{q} + \left(\frac{L}{2} + (\mathbf{b}_u^{\mathrm{T}} + h\mathbf{b}_\theta^{\mathrm{T}} + 2\xi h\mathbf{c}_\theta^{\mathrm{T}})\mathbf{q}\right)\ddot{\xi} = 0 \end{aligned} \tag{13}$$

where the velocity $\dot{x} = (L/2)\dot{\xi}$ and acceleration $\ddot{x} = (L/2)\ddot{\xi}$ of the truss-oscillator contact point can be obtained.

Multiplying Eq. (13) with $L/2$ and writing the resultant equation in the following form

$$\ddot{x} = \boldsymbol{\varphi}^{\mathrm{T}}\ddot{\mathbf{q}} + \chi \tag{14}$$

where

$$\boldsymbol{\varphi} = -\frac{\mathbf{a}_u + h\mathbf{a}_\theta + \xi(\mathbf{b}_u + h\mathbf{b}_\theta) + \xi^2 h\mathbf{c}_\theta}{1 + \dfrac{2}{L}(\mathbf{b}_u + h\mathbf{b}_\theta + 2\xi h\mathbf{c}_\theta)^{\mathrm{T}}\mathbf{q}} \tag{15}$$

$$\chi = -\frac{\dfrac{4h\dot{x}^2}{L}\mathbf{c}_\theta^{\mathrm{T}}\mathbf{q} + 2\dot{x}(\mathbf{b}_u + h\mathbf{b}_\theta + 2\xi h\mathbf{c}_\theta)^{\mathrm{T}}\dot{\mathbf{q}}}{\dfrac{L}{2} + (\mathbf{b}_u + h\mathbf{b}_\theta + 2\xi h\mathbf{c}_\theta)^{\mathrm{T}}\mathbf{q}} \tag{16}$$

Eq. (14) relates the horizontal coordinate corresponding to the location of the moving oscillator to the modal coordinates of the truss structure.

4. Dynamic model of the whole system

The equations of motion for the sprung and unsprung masses of the oscillator (Fig. 3) are

$$m_z\ddot{z} = W_z - f_{zy} \tag{17}$$

$$m_y\ddot{y} = W_y + f_{zy} + f_c \tag{18}$$

where

$$f_{zy} = c(\dot{z} - \dot{y}) + k(z - y) \tag{19}$$

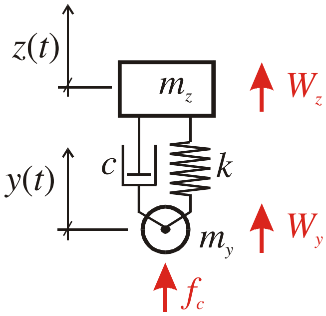

Fig. 3. The moving oscillator.

and $W_z = -m_z g$ and $W_y = -m_y g$ are the weights of the two masses, in which g is the gravitational constant. f_c is the dynamic contact force at the oscillator–truss contact point (the moving load from the oscillator acting onto the truss).

The equation of motion for the truss, Eq. (3), can be decoupled using the FE modes and then transformed into an equation in the modal coordinator vector as

$$\ddot{\mathbf{q}} + \mathrm{diag}[\omega^2]\mathbf{q} = -f_c(t)\boldsymbol{\psi}_w(x) \tag{20}$$

where $\mathrm{diag}[\omega^2]$ is a diagonal matrix of appropriate dimension whose diagonal elements are the natural frequencies squared of the truss structure ranked in ascending order, and x (or ξ) is the truss-oscillator contact point coordinate obtained from Eq. (10). Notice that $\boldsymbol{\psi}^{\mathrm{FE}}\mathbf{f} = -f_c\boldsymbol{\psi}_w$ is used in the derivation of the right-hand side of Eq. (20). If damping is present in the truss and the damping matrix $\mathbf{C}$ can be expressed by $\alpha\mathbf{M} + \beta\mathbf{K}$ or $\mathbf{C} = \sum_i \beta_i \mathbf{K}^{i-1}$ (where α and β are constants and i is an integer), or $\mathbf{CM}^{-1}\mathbf{K} = \mathbf{KM}^{-1}\mathbf{C}$, Eq. (3) can still be decoupled [27]. It would have an additional damping term though.

It is assumed that if the unsprung mass is in contact with the truss, its vertical displacement equals the deflection of the beam at the location represented by the un-deformed coordinate x, that is

$$y(t) = \mathbf{q}^{\mathrm{T}}(t)\boldsymbol{\psi}_w(x) \tag{21}$$

and therefore

$$\dot{y} = \dot{\mathbf{q}}^{\mathrm{T}}\boldsymbol{\psi} + \mathbf{q}^{\mathrm{T}}\boldsymbol{\psi}'_w\dot{x} \tag{22}$$

$$\ddot{y} = \ddot{\mathbf{q}}^{\mathrm{T}}\boldsymbol{\psi}_w + 2\dot{\mathbf{q}}^{\mathrm{T}}\boldsymbol{\psi}'_w\dot{x} + \mathbf{q}^{\mathrm{T}}\boldsymbol{\psi}''_w\dot{x}^2 + \mathbf{q}^{\mathrm{T}}\boldsymbol{\psi}'_w\ddot{x} \tag{23}$$

where the prime represents differentiation with respect to x.

From Eqs. (18) and (20) it follows that

$$\ddot{\mathbf{q}} + \mathrm{diag}[\omega^2]\mathbf{q} = (W_y + f_{zy} - m_y\ddot{y})\boldsymbol{\psi}_w \tag{24}$$

By substituting Eqs. (14) and (23) into Eq. (24), one gets

$$[\mathbf{I} + m_y\boldsymbol{\psi}_w\boldsymbol{\psi}_w^{\mathrm{T}} + m_y\boldsymbol{\psi}_w\boldsymbol{\psi}_w'^{\mathrm{T}}\mathbf{q}\boldsymbol{\phi}^{\mathrm{T}}]\ddot{\mathbf{q}} = \boldsymbol{\psi}_w(W_y + f_{zy}) - \mathrm{diag}[\omega^2]\mathbf{q} - m_y\boldsymbol{\psi}_w(2\dot{\mathbf{q}}^{\mathrm{T}}\boldsymbol{\psi}'_w\dot{x} + \mathbf{q}^{\mathrm{T}}\boldsymbol{\psi}''_w\dot{x}^2 + \mathbf{q}^{\mathrm{T}}\boldsymbol{\psi}'_w\chi) \tag{25}$$

where $\mathbf{I}$ is identity matrix of appropriate dimension. Eqs. (11), (12), (17)–(19), and (25) must be solved simultaneously to obtain the vibration of the truss and the oscillator. Even though Eq. (25) is nonlinear, the degree of nonlinearity is small as the contribution from the axial displacement and the rotation of the beam cross-section is small. Eq. (25) is solved by using Runge–Kutta algorithm (ode45) available in MATLAB and capable of dealing with nonlinear differential equations.

The proposed model considers the influence of the horizontal displacement and the rotation of the cross-section of the component beams of the truss when it is excited by a moving oscillator in contact. If these displacements of the top fibre of the beams of the top deck are ignored, the above equations still apply when the condition $x^* = vt = x$ is imposed. As a result of this omission, Eq. (25)

reduces to

$$[\mathbf{I} + m_y \boldsymbol{\psi}_w \boldsymbol{\psi}_w^{\mathrm{T}}]\ddot{\mathbf{q}} = \boldsymbol{\psi}_w (W_y + f_{zy}) - \mathrm{diag}[\omega^2]\mathbf{q} - m_y \boldsymbol{\psi}_w (2\dot{\mathbf{q}}^{\mathrm{T}} \boldsymbol{\psi}'_w v + \mathbf{q}^{\mathrm{T}} \boldsymbol{\psi}''_w v^2) \tag{26}$$

5. Numerical results

A numerical example of the truss shown in Fig. 1 is analysed. It has the following material and geometric data: $EI = 6.3 \times 10^6\,\mathrm{Nm}^2$, $EA = 6.3 \times 10^9\,\mathrm{N}$, the shear modulus is 81 GPa and the shear factor is 0.9, $L_b = 50\,\mathrm{m}$, $m_y = 100\,\mathrm{kg}$, $m_z = 1000\,\mathrm{kg}$, $k = 3.95 \times 10^6\,\mathrm{N/m}$, $c = 25130\,\mathrm{Ns/m}$, $\rho A = 225\,\mathrm{kg/m}$. There are six beams of equal length in the top deck. The height is 7.217 m. The critical speed of the truss $v_{\mathrm{cr}} = 35.34\,\mathrm{m/s}$, which is defined as the ratio of the fundamental frequency in Hz ($\omega_1/2\pi$) of the truss to the lowest wave number of a beam in the top deck. It is found that eight Timoshenko elements for each beam component already gives converging results and therefore are used throughout the numerical analysis work.

All the dynamic values of the system are non-dimensionalised against the relevant static values when presented in the figures below. The non-dimensionalised contact force between the moving oscillator and the truss is shown in Fig. 4. It turns out that the difference in the dynamic contact force between the model with and without the influence of u and θ is very small, as displayed by the non-dimensionalised absolute error in Fig. 5. The non-dimensionalised displacement of the contact point is shown in Fig. 6, while the difference (non-dimensionalised absolute error) in the dynamic response between the models with and without the influence of u and θ is given in Fig. 7, where w_{st} is the mid-span static deflection of the top deck when the oscillator is located at that same position. Again it can be seen that the difference in the results between the models with and without the influence of u and θ is negligibly small. Therefore this influence can be safely ignored and are not included in the subsequent computation.

Numerical results of $y(t)/w_{\mathrm{st}}$ and $z(t)/z_{\mathrm{st}}$ at various speeds of v are given in Figs. 8 and 9, respectively, where z_{st} is the static deflection of the sprung mass. It can be seen from Fig. 8 that at very low v, the vertical motion of the unsprung mass is small. It is actually nearly equal to the static deflection of the truss at various locations (the influence line). As v becomes higher, the vertical motion of the unsprung mass grows bigger in general. At around the critical speed, the maximum vibration is more than twice as much as the maximum static

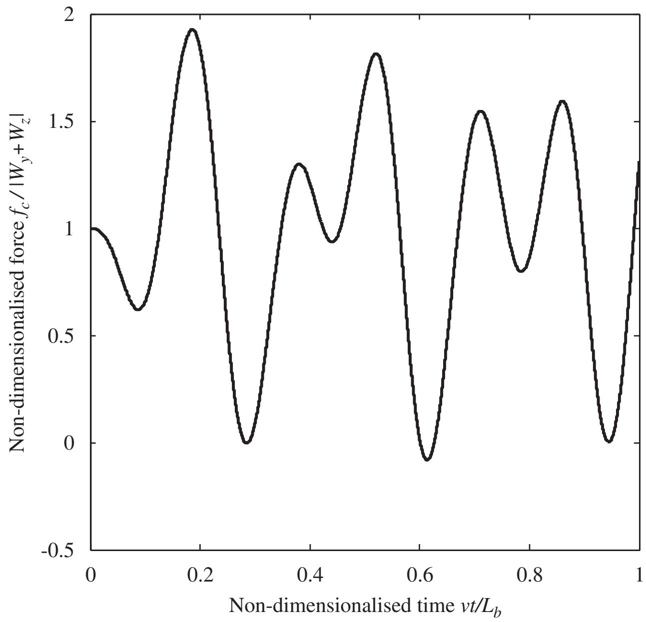

Fig. 4. Dynamic contact force.

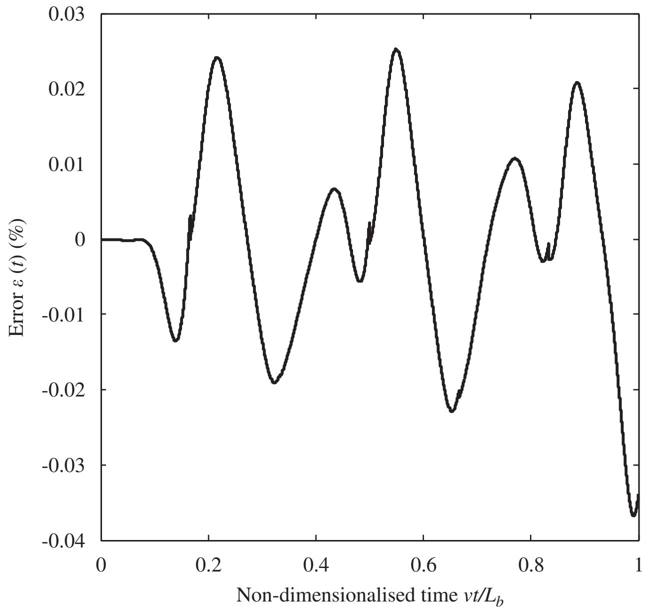

Fig. 5. Difference between dynamic contact forces with and without horizontal motion and beam rotation.

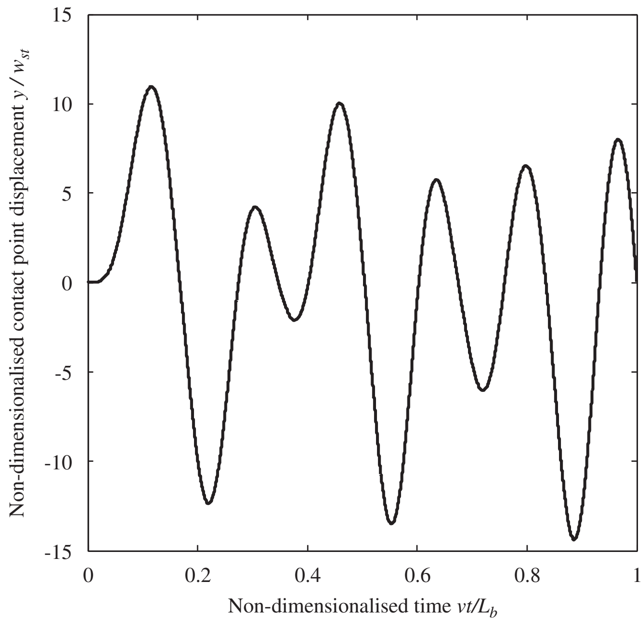

Fig. 6. Non-dimensionalised dynamic deflection of the contact point.

deflection of the truss. But at very high speeds, there is little motion of the unsprung mass and of the truss since the oscillator moves so fast that the structure has hardly time to respond to the excitation of the moving oscillator before it runs off the truss. As for the sprung mass, the parameter values chosen result in very little variation of its motion in relation to its static value and hence afford a comfortable ride. The online version of this article contains the animations of vibration of the system at three speeds (Annex 1: $v = 0.5v_{\mathrm{cr}}$; Annex 2: $v = 1.06v_{\mathrm{cr}}$; Annex 3: $v = 4v_{\mathrm{cr}}$).

Numerical results of $f_c/(W_y + W_z)$ are shown in Fig. 10. Parameter values used are the same as in the previous case, except that $k = 8.88 \times 10^3\,\mathrm{N/m}$, $c = 1192\,\mathrm{Ns/m}$ and $\rho A = 1125\,\mathrm{kg/m}$. They are chosen in such

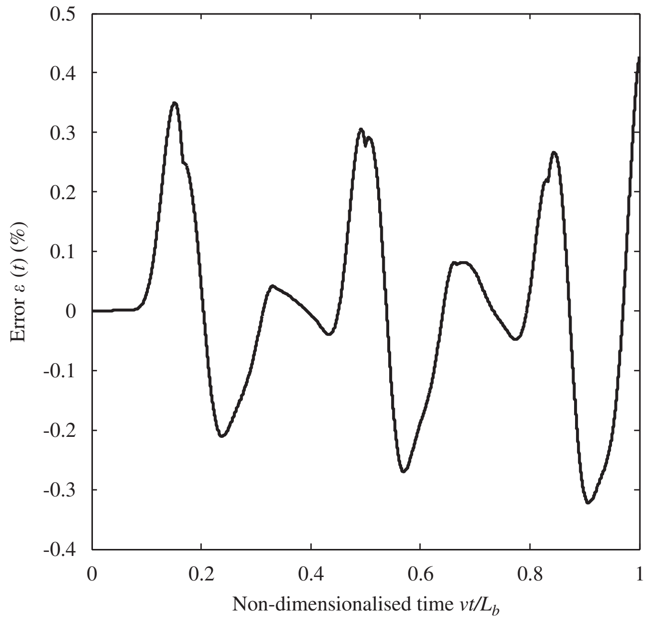

Fig. 7. Difference in the dynamic deflections with and without horizontal displacement and beam rotation.

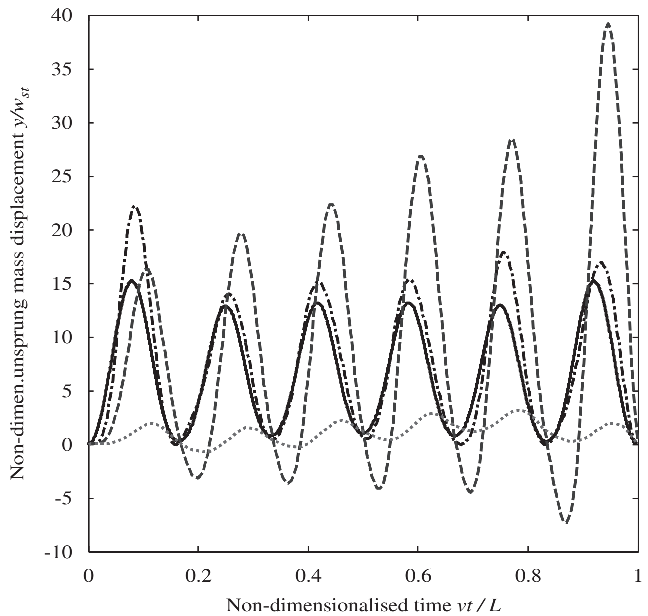

Fig. 8. $y(t)/w_{st}$ at various speeds (—: $v/v_{cr} \approx 0$; - · -: $v/v_{cr} = 0.5$; - - -: $v/v_{cr} = 1.06$; ….: $v/v_{cr} = 4$).

a way that the dynamic contact force is very close to its static value. An example showing large dynamic contact force is given in Fig. 11, where the spring stiffness has been increased to $k = 4.93 \times 10^6$ N/m and the viscous property of the damper is $c = 2800$ Ns/m. The dynamic contact force is shown to become negative at around $vt/L = 0.9$. It is clear from Fig. 11 that if the oscillator slides along the top deck of the truss, then it loses contact toward the end of its travel on the truss. Separation of the moving structure from and its subsequent reattachment to the supporting structure was studied for a moving-mass problem in Ref. [28] and

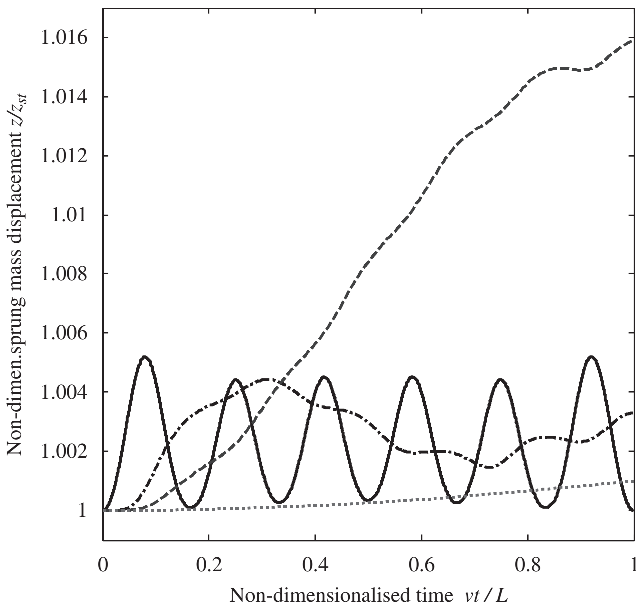

Fig. 9. $z(t)/z_{\mathrm{st}}$ at various speeds (—: $v/v_{\mathrm{cr}} \approx 0$; - · -: $v/v_{\mathrm{cr}} = 0.5$; - - -: $v/v_{\mathrm{cr}} = 1.06$; ….: $v/v_{\mathrm{cr}} = 4$).

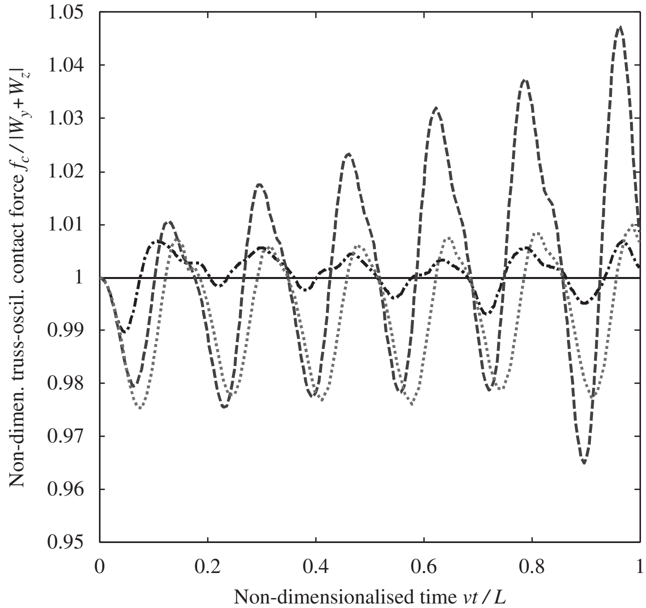

Fig. 10. $f_c/(W_y + W_z)$ at various speeds (—: $v/v_{\mathrm{cr}} \approx 0$; - · -: $v/v_{\mathrm{cr}} = 0.5$; - - -: $v/v_{\mathrm{cr}} = 1.06$; ….: $v/v_{\mathrm{cr}} = 4$).

for a moving oscillator problem in Refs. [29,30]. As they are very complicated to study, these two topics are not pursued further here.

6. Conclusions

This paper studies the oscillator–truss coupled dynamic response when the oscillator moves on the truss structure. It presents an analytical–numerical combined approach that takes advantage of both methods. The formulation considers the horizontal variations of the oscillator–truss contact point due to the horizontal

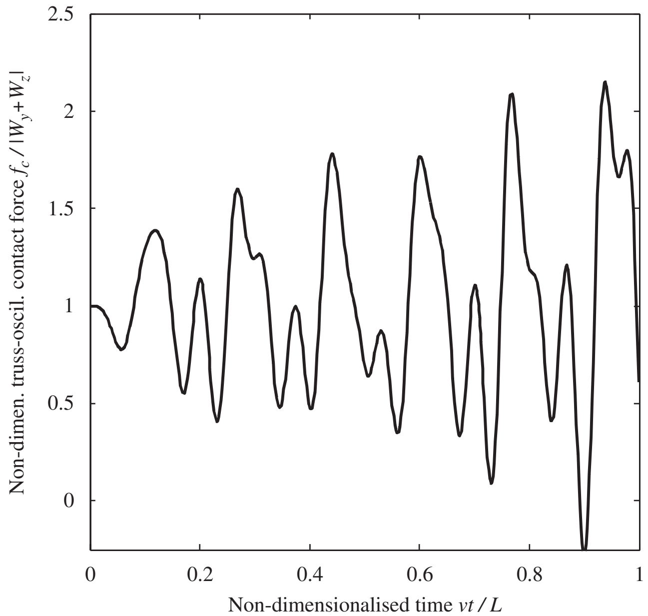

Fig. 11. $f_c/(W_y + W_z)$ at $v/v_{cr} = 1.06$.

motion of the truss and the rotation of the beam section. The numerical results for a deck truss show that the dynamic deflection of the truss can be several times higher than the maximum static deflection and the moving load (dynamic contact force) can also be a few times greater than the static force (self-weight of the oscillator). However, by using suitably chosen parameter values, the dynamic response (of the oscillator or the beam) and the dynamic contact force can be brought very close to its static value over a very wide speed range and hence allow a comfortable ride if the oscillator represents a vehicle.

It is found that there is only a negligible influence of the horizontal motion and the beam rotation on the dynamic response from the examples studied. The methodology is still applicable to vibration problems where there is a strong coupling between vertical and horizontal displacements.

Acknowledgements

This research is conducted at the Department of Engineering, University of Liverpool and is sponsored by the RSB funding of the Department and EPSRC of the UK (Ref. EP/D057671/01: Moving-load Distributions in Structural Dynamics). The first author is sponsored by Projects T79/2006 (Ministerio de Fomento—Metro de Madrid—CDM) and TRA2007-67167 (Ministerio de Educación y Ciencia—FEDER).

The authors are also grateful to the referees and the Associate Editor for their valuable comments that have helped improve the paper.

Appendix A

To demonstrate the methodology proposed in this paper, a continuous Euler beam resting on multiple supports with classical (pinned, free or clamped) boundary conditions is used. The closed-form analytical modes of such a beam can be obtained after solving a highly nonlinear transcendental equation in the frequencies of the beam [31]. There is not a single mathematical expression for a mode and each mode is defined span-wise. A mode satisfies the left and right boundary conditions and is continuous (also its derivatives) at the intermediate support(s).

Take a two-span beam shown in Fig. A1 as an example.

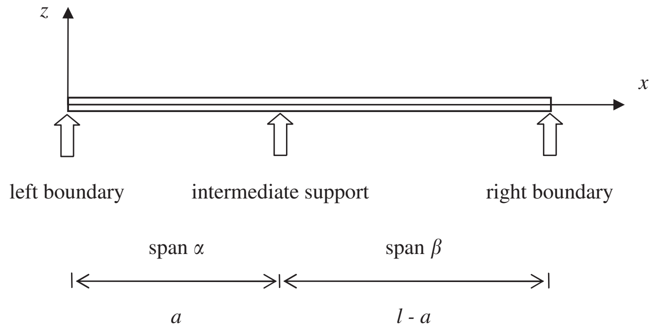

Fig. A1. A two-span continuous beam.

The i-th analytical mode of the whole beam may be expressed as

$$\varphi_i(\xi) = \begin{cases} \varphi_{i\alpha}(\xi), & 0 \leqslant \xi \leqslant \mu \\ \varphi_{i\beta}(\xi), & \mu \leqslant \xi \leqslant 1 \end{cases} \tag{A.1}$$

where $\xi = x/l$.

The i-th and j-th modes of the whole beam satisfies the following equations

$$EI\varphi_i''''(\xi) - \omega_i^2 \rho A l^4 \varphi_i(\xi) = 0, \quad 0 \leqslant \xi \leqslant 1 \tag{A.2}$$

$$EI\varphi_j''''(\xi) - \omega_j^2 \rho A l^4 \varphi_j(\xi) = 0, \quad 0 \leqslant \xi \leqslant 1 \tag{A.3}$$

The prime stands for derivative with respect to ξ. It is needless to say that the eigenvalue equations. (A.2) and (A.3) apply to the whole beam and any spans of the beam.

It can be derived that

$$\begin{aligned} \int_0^1 \varphi_j(\xi)\varphi_i''''(\xi)\,\mathrm{d}\xi &= \int_0^\mu \varphi_{j\alpha}(\xi)\varphi_{i\alpha}''''(\xi)\,\mathrm{d}\xi + \int_\mu^1 \varphi_{j\beta}(\xi)\varphi_{i\beta}''''(\xi)\,\mathrm{d}\xi \\ &= [\varphi_{j\alpha}(\xi)\varphi_{i\alpha}'''(\xi)]_0^\mu - \int_0^\mu \varphi_{j\alpha}'(\xi)\varphi_{i\alpha}'''(\xi)\,\mathrm{d}\xi + [\varphi_{j\beta}(\xi)\varphi_{i\beta}'''(\xi)]_\mu^1 - \int_\mu^1 \varphi_{j\beta}'(x)\varphi_{i\beta}'''(\xi)\,\mathrm{d}\xi \\ &= [\varphi_{j\alpha}(\xi)\varphi_{i\alpha}'''(\xi)]_0^\mu - [\varphi_{j\alpha}'(\xi)\varphi_{i\alpha}''(\xi)]_0^\mu + \int_0^\mu \varphi_{j\alpha}''(\xi)\varphi_{i\alpha}''(\xi)\,\mathrm{d}\xi + [\varphi_{j\beta}(\xi)\varphi_{i\beta}'''(\xi)]_\mu^1 \\ &\quad - [\varphi_{j\beta}'(\xi)\varphi_{i\beta}''(\xi)]_\mu^1 + \int_\mu^1 \varphi_{j\beta}''(\xi)\varphi_{i\beta}''(\xi)\,\mathrm{d}\xi = \int_0^1 \varphi_j''(\xi)\varphi_i''(\xi)\,\mathrm{d}\xi \end{aligned}$$

where $\mu = a/l$. Note that in the above derivation, $[\varphi_{j\alpha}(\xi)\varphi_{i\alpha}'''(\xi)]_0 = 0$, $[\varphi_{j\alpha}'(\xi)\varphi_{i\alpha}''(\xi)]_0 = 0$, $[\varphi_{j\beta}(\xi)\varphi_{i\beta}'''(\xi)]^1 = 0$, $[\varphi_{j\beta}'(\xi)\varphi_{i\beta}''(\xi)]^1 = 0$ as all modes satisfy the left and right (classical) boundary conditions, and $[\varphi_{j\alpha}(\xi)\varphi_{i\alpha}'''(\xi)]^\mu + [\varphi_{j\beta}(\xi)\varphi_{i\beta}'''(\xi)]_\mu = 0$ and $[\varphi_{j\alpha}'(\xi)\varphi_{i\alpha}''(\xi)]^\mu + [\varphi_{j\beta}'(\xi)\varphi_{i\beta}''(\xi)]_\mu = 0$ due to displacement continuity at the intermediate support.

Similarly, it can be derived that $\int_0^1 \varphi_i(\xi)\varphi_j''''(\xi)\,\mathrm{d}\xi = \int_0^1 \varphi_i''(\xi)\varphi_j''(\xi)\,\mathrm{d}\xi$.

Multiplying both sides of Eq. (A.2) by $\varphi_j(\xi)$ and Eq. (A.3) by $\varphi_i(\xi)$, then integrating the resultant equations over [0, 1] and then taking away one equation from the other, yields the following relationship:

$$\rho A l^4(\omega_i^2 - \omega_j^2)\int_0^1 \varphi_i(\xi)\varphi_j(\xi)\,\mathrm{d}\xi = 0 \tag{A.4}$$

Therefore it may be concluded that for any two distinct frequencies ω_i and ω_j

$$\int_0^1 \varphi_i(\xi)\varphi_j(\xi)\,\mathrm{d}\xi = 0 \quad (\text{when } i \neq j) \tag{A.5}$$

which means that the analytical modes of the whole beam of any two distinct frequencies are orthogonal to one another.

Appendix B. Supporting Information

Supplementary data associated with this article can be found in the online version at doi:10.1016/j.jsv.2008.09.049.

References

[1] J.E. Akin, M. Mofid, Numerical solution for response of beams with moving mass, *ASCE Journal of Structural Engineering* 115 (1989) 120–131.
[2] S. Marchesiello, A. Fasana, L. Garibaldi, B.A.D. Piombo, Dynamics of multi-span continuous straight bridges subject to multi-degrees of freedom moving vehicle excitation, *Journal of Sound and Vibration* 224 (1999) 541–561.
[3] P.K. Chatterjee, T.K. Datta, C.S. Surana, Vibration of continuous bridges under moving vehicles, *Journal of Sound and Vibration* 169 (1994) 619–632.
[4] B. Yang, A.A. Tan, L.A. Bergman, Direct numerical procedure for solution of moving oscillator problems, *ASCE Journal of Engineering Mechanics* 126 (2000) 462–469.
[5] A.V. Metrikine, S.N. Verichev, Instability of vibration of a moving oscillator on a flexibly supported Timoshenko beam, *Archive of Applied Mechanics* 71 (9) (2001) 613–624.
[6] L. Fryba, *Vibrations of the Solids and Structures under Moving Loads*, Thomas Telford Publishing House, 1999.
[7] H. Ouyang, J.E. Mottershead, A numerical–analytical combined method for vibration of a beam excited by a moving flexible body, *International Journal for Numerical Methods in Engineering* 72 (2007) 1181–1191.
[8] L. Fryba, Impacts of two-axle system traversing a beam, *International Journal of Solid and Structures* 4 (1968) 1107–1123.
[9] P. Lou, A vehicle–track–bridge interaction element considering vehicle's pitching effect, *Finite Elements in Analysis and Design* 41 (2005) 397–427.
[10] Y.K. Cheung, F.T.K. Au, D.Y. Zheng, Y.S. Cheng, Vibration of multi-span non-uniform bridges under moving vehicles and trains using modified beam vibration functions, *Journal of Sound and Vibration* 228 (1999) 611–628.
[11] P.K. Chatterjee, T.K. Datta, C.S. Surana, Vibration of suspension bridges under vehicular movement, *Journal of Structural Engineering* 120 (3) (1994) 681–703.
[12] R.T. Wang, J.S. Lin, Vibration of multi-span Timoshenko frames due to moving loads, *Journal of Sound and Vibration* 212 (1998) 417–434.
[13] D.Z. Huang, T.L. Wang, Vibration of highway steel bridges with longitudinal grades, *Computers and Structures* 69 (2) (1998) 235–245.
[14] J.L. Humar, A.H. Kashif, Dynamic response analysis of slab-type bridges, *Journal of Structural Engineering* 121 (1) (1995) 48–62.
[15] K. Henchi, M. Fafard, M. Talbort, G. Dhatti, An efficient algorithm for dynamic analysis of bridge under moving vehicles using coupled modal and physical components approach, *Journal of Sound and Vibration* 212 (4) (1998) 663–683.
[16] J.D. Yau, Y.B. Yang, Vibration reduction for cable-stayed bridges traveled by high-speed trains, *Finite Elements in Analysis and Design* 40 (2004) 341–359.
[17] S.-Y. Lee, S.-S. Yhim, Dynamic behavior of long-span box girder bridges subjected to moving loads: numerical analysis and experimental verification, *International Journal of Solids and Structures* 42 (2005) 5021–5035.
[18] F.T.K. Au, Y.S. Cheng, Y.K. Cheung, Vibration analysis of bridges under moving vehicles and trains: an overview, *Progress in Structural Engineering and Materials* 3 (2001) 299–304.
[19] Y.B. Yang, J.D. Yau, Y.S. Wu, *Vehicle– Bridge Interaction Dynamics*, World Scientific Publishing Co., Singapore, 2004.
[20] M. Géradin, D. Rixen, *Mechanical Vibrations: Theory and Application to Structural Dynamics*, Wiley, Chichester, 1997.
[21] F.J. Fuenmayor, J.L. Restrepo, J.E. Tarancón, L. Baeza, Error estimation and h-adaptive refinement in the analysis of natural frequencies, *Finite Elements in Analysis and Design* 38 (2) (2001) 137–153.
[22] R.D. Blevins, *Formulas for Natural Frequency and Mode Shape*, Krieger, Malabar, 1984.
[23] P.J.P. Gonçalves, M.J. Brennan, S.J. Elliott, Numerical evaluation of high-order modes of vibration in uniform Euler–Bernoulli beams, *Journal of Sound and Vibration* 301 (2007) 1035–1039.
[24] S.M. Han, H. Benaroya, T. Wei, Dynamics of transversely vibrating beams using four engineering theories, *Journal of Sound and Vibration* 225 (5) (1999) 935–988.
[25] J.S. Przemieniecki, *Theory of Matrix Structural Analysis*, McGraw-Hill, New York, 1968.
[26] D. Hochlenert, G. Spelsberg-Korspeter, P. Hagedorn, Friction induced vibrations in moving continua and their application to brake squeal, *Journal of Applied Mechanics* 74 (2007) 542–549.
[27] D.J. Inman, *Vibration with Control*, Wiley, Chichester, 2006.
[28] U. Lee, Separation between the flexible structure and the moving mass sliding on it, *Journal of Sound and Vibration* 209 (5) (1998) 867–877.

[29] Y.S. Cheng, F.T.K. Au, Y.K. Cheung, D.Y. Zheng, On the separation between the moving vehicle and bridge, *Journal of Sound and Vibration* 222 (5) (1999) 781–801.
[30] D. Stancioiu, H. Ouyang, J.E. Mottershead, Vibration of a beam excited by a moving oscillator considering separation and reattachment, *Journal of Sound and Vibration* 310 (4–5) (2007) 1128–1140.
[31] S. Timoshenko, *Vibration Problems in Engineering*, third ed., Van Nostrand, New York, 1955.